Cosmic strings in a space–time with positive cosmological constant

Yves Brihaye [a], Betti Hartmann [b],*

[a] *Faculté de Sciences, Université de Mons-Hainaut, 7000 Mons, Belgium*
[b] *School of Engineering and Science, Jacobs University Bremen, 28759 Bremen, Germany*

A R T I C L E   I N F O

A B S T R A C T

We study Abelian strings in a fixed de Sitter background. We find that the gauge and Higgs fields extend smoothly across the cosmological horizon and that the string solutions have oscillating scalar fields outside the cosmological horizon for all currently accepted values of the cosmological constant. If the gauge to Higgs boson mass ratio is small enough, the gauge field function has a power-like behaviour, while it is oscillating outside the cosmological horizon if Higgs and gauge boson mass are comparable. Moreover, we observe that Abelian strings exist only up to a maximal value of the cosmological constant and that two branches of solutions exist that meet at this maximal value. We also construct radially excited solutions that only exist for non-vanishing values of the cosmological constant and are thus a novel feature as compared to flat space–time. Considering the effect of the de Sitter string on the space–time, we observe that the deficit angle increases with increasing cosmological constant. Lensed objects would thus be separated by a larger angle as compared to asymptotically flat space–time.

1. Introduction

Topological defects are believed to have formed during the phase transitions in the early universe. While magnetic monopoles and domain walls are catastrophic for the universe since they overclose it, cosmic strings [1] were believed to be important for the structure formation for a long time. Recent Cosmic Microwave background (CMB) measurements however excluded cosmic strings as seeds for structure formation [2].

In recent years, cosmic strings have been linked to the fundamental superstrings of string theory and this has boosted renewed interest in these objects. The low energy limit of certain string theories contain so-called F- and D-strings, where "F" stands for fundamental and "D" for Dirichlet. It was also realized that supersymmetric bound states of F- and D-strings exist, so-called (p,q)-strings [3]. The formation of networks of such strings has been discussed in a variety of string-inspired, hybrid inflation models [4] and the signatures of such networks in the CMB anisotropies have been investigated [5].

A field theoretical model that contains string-like defects is the Abelian Higgs model [6]. Abelian Higgs strings are infinitely extended with a core radius inversely proportional to the Higgs boson mass and magnetic flux tubes with radius inversely proportional to the gauge boson mass. Recently, two copies of the Abelian

Higgs model interacting via a potential term have been discussed as field-theoretical realizations of (p,q)-strings [7].

The gravitational effects of Abelian strings have also been investigated [8]. The main observation is that the space–time far away from the string is conical, i.e., contains a deficit angle. The consequence of this is that cosmic strings would act as gravitational lenses, which opens a possibility to detect them indirectly [9].

Since diverse astrophysical observations, e.g., redshift measurements of type Ia supernovae [10] lead to the assumption that our universe is dominated by a form of dark energy, a positive cosmological constant, it is surely of interest to understand the effects of a positive cosmological constant on cosmic string solutions. That the effect of a positive cosmological constant is non-trivial has been shown, e.g., in the study of cosmic string loops, which form unavoidably in the evolution of cosmic string networks. While cosmic string loops collapse under their own tension in space–times with Minkowski or Robertson–Walker metric, this is not the case for large loops in de Sitter space–time [11]. Thus string loops can survive in space–times with positive cosmological constant.

Moreover, the so-called "de Sitter/Conformal Field Theory" (dS/CFT) correspondence [12] suggests a holographic duality between a d-dimensional dS space and a conformal field theory "living" on the boundary of dS.

The properties of Abelian strings in de Sitter space–time have been discussed using analytic tools [13] as well as numerical ones [14,15]. In [14], a model describing Abelian strings coupled minimally to gravity including a positive cosmological constant have been studied. While this model describes the interaction of the matter fields with the gravitational fields properly, the space–time

* Corresponding author.
  E-mail addresses: yves.brihaye@umh.ac.be (Y. Brihaye),
b.hartmann@jacobs-university.de (B. Hartmann).

was assumed to have the same symmetries as the string, namely, it was assumed to be cylindrically symmetric. However, the space–time describing our universe with positive cosmological constant is genuinely spherically symmetric for an inertial observer. Thus, it is, e.g., not difficult to study spherically symmetric topological defects such as magnetic monopoles in a spherically symmetric de Sitter space [16], while it becomes more difficult if one tries to study objects with symmetry different from spherical symmetry. It was, however, realized in [15,17] that if one studies strings in a fixed (anti-)de Sitter background that the equations describing this situation become ordinary differential equations if one assumes that the fields of the string depend only on a specific combination of the spherical coordinates.

Abelian strings have been studied in a background space–time with positive cosmological constant before [15]. In this Letter, we reinvestigate the solutions given in [15]. The authors of [15] have constructed these solutions (in static coordinates) only inside the cosmological horizon, while we show here that they extend smoothly across the cosmological horizon. We also present the asymptotic behaviour of the solutions, which is qualitatively similar to that of magnetic monopoles in de Sitter space [16]. Our results indicate that for all currently accepted values of the cosmological constant, the solutions have oscillating scalar fields outside the horizon. Moreover, we present new, radially excited solutions that do not exist in the flat space–time limit.

Our Letter is organized as follows: in Section 2, we give the model and equations of motion, while in Section 3, we present the asymptotic behaviour of the solutions. In Section 4, we discuss our numerical results and conclude in Section 5.

2. The model

We study Abelian strings in a fixed de Sitter background. The metric of the background in static, spherical coordinates (representing the coordinates of an inertial observer) can be parametrized as follows:

$$ds^2 = -\left(1 - \frac{r^2}{l^2}\right)dt^2 + \left(1 - \frac{r^2}{l^2}\right)^{-1}dr^2 + r^2\left(d\theta^2 + \sin^2\theta\, d\varphi^2\right),$$

where $l = \sqrt{3/\Lambda}$ is the de Sitter radius and Λ is the (positive) cosmological constant.

The Lagrangian for the Abelian strings reads [6]:

$$\mathcal{L} = -\frac{1}{4}F_{\mu\nu}F^{\mu\nu} - (D_\mu\phi)^*D^\mu\phi - \frac{\beta}{4}(\phi^*\phi - \eta^2)^2,$$

with the field strength tensor $F_{\mu\nu} = \partial_\mu A_\nu - \partial_\nu A_\mu$ of the $U(1)$ gauge field and the covariant derivative $D_\mu\phi = \partial_\mu\phi - ieA_\mu\phi$ of a with coupling constant e minimally coupled complex scalar field ϕ. The Lagrangian is invariant under a local $U(1)$. When ϕ attains a non-vanishing vacuum expectation value η, the symmetry breaks down from $U(1)$ to 1. The particle content of the theory is then a massive gauge boson with mass $M_W = e\eta$ and a massive scalar field (the Higgs field) with mass $m_H = \sqrt{2\beta}\eta$.

The ansatz for the gauge and Higgs fields parametrized in spherical coordinates (r, θ, φ) reads:

$$A_t = A_r = A_\theta = 0, \qquad A_\varphi = \frac{1}{e}\big(n - P(r,\theta)\big), \qquad \phi = \eta f(r,\theta)e^{in\varphi},$$

where n is an integer, which corresponds to the winding number of the string.

We want to study cylindrical configurations here and thus assume that in the following the matter field functions P and f depend only on the specific combination $r\sin\theta \equiv \rho$. The partial

differential equations then reduce to ordinary differential equations that depend only on the coordinate ρ and in the limit $l \to \infty$ correspond to the equations of the Abelian string [6].

2.1. The equations and boundary conditions

Varying the Lagrangian with respect to the gauge and Higgs fields gives the Euler–Lagrange equations, which here reduce to ordinary differential equations for the field functions P and f. These equations describe a cylindrical, string-like configuration in a fixed de Sitter background and read:

$$\left(1 - \frac{\rho^2}{l^2}\right)P'' = 2\eta^2 e^2 Pf^2 + \frac{P'}{\rho}\left(1 + \frac{2\rho^2}{l^2}\right),$$

for the gauge field function and

$$\left(1 - \frac{\rho^2}{l^2}\right)f'' = \frac{\beta}{2}\eta^2 f(f^2 - 1) - \frac{f'}{\rho}\left(1 - \frac{4\rho^2}{L^2}\right) + \frac{P^2 f}{\rho^2},$$

for the Higgs field function, where the prime denotes the derivative with respect to ρ.

One can use rescaled coordinates and quantities and define

$$x = \sqrt{\beta}\eta\rho, \qquad \alpha = \frac{2M_W^2}{M_H^2} = \frac{e^2}{\beta}, \qquad L = \sqrt{\beta}\eta l.$$

The equations then depend only on the parameters L and α, where the half of the latter represents the square of ratio of the gauge boson mass to Higgs boson mass. Note that with this rescaling, we "measure" the cosmological constant in units of the square of the Higgs boson mass. Furthermore, the case $L \to \infty$ and $\alpha = 0.5$ corresponds to the self-dual, i.e., BPS limit.

The positive cosmological constant leads to the presence of a cosmological horizon at $\rho = l$, i.e., $x = L$. Here, we impose boundary conditions at $x = L$ such that the matter fields are regular at this cosmological horizon. Numerically, we first integrate the equations on the interval $x \in [0 : L]$ subject to the following boundary conditions:

$$P(0) = n, \qquad f(0) = 0, \qquad \left[2\alpha x Pf^2 + 3P'\right]_{x=L} = 0,$$
$$\left[x^2 f(f^2 - 1) + 6xf' + 2P^2 f\right]_{x=L} = 0.$$

In a second step, we integrate the equations for $x \in [L, \infty]$ by using as initial conditions the numerical values $P(L)$, $P'(L)$, $f(L)$, $f'(L)$ obtained during the integration for $x \in [0 : L]$. We then match the solution for $x \in [0 : L]$ and for $x \in [L : \infty]$ at the horizon $x = L$.

The energy density $\epsilon = -T_0^0$ reads:

$$\epsilon = \eta^4\left[\left(1 - \frac{x^2}{L^2}\right)(f')^2 + \left(1 - \frac{x^2}{L^2}\right)\frac{1}{2\alpha}\frac{(P')^2}{x^2} + \frac{P^2 f^2}{x^2} + \frac{1}{4}(1 - f^2)^2\right].$$

The inertial mass per unit length inside the cosmological horizon, M_{in}, can then be defined by integrating T_0^0 over a section of constant z, leading to

$$M_{in} = 2\pi\eta^2\int_0^L dx\, x T_0^0.$$

3. Asymptotic behaviour

The asymptotic behaviour of the solutions of Eqs. (4), (5) plays a major role in the discussion and depends crucially on the signs of two dimensionless combinations of the mass scales of the theory, namely on $R_1 \equiv 1 - 8\alpha L^2$ and $R_2 \equiv 9 - 4L^2$. We discuss the different cases separately.

1. For $R_1 > 0$ and $R_2 > 0$, we have

$$P(x \gg 1) = P_0 x^c, \quad c = \frac{-1 \pm \sqrt{R_1}}{2}, \tag{10}$$

$$f(x \gg 1) = 1 - F_0 x^d, \quad d = \frac{-3 \pm \sqrt{R_2}}{2}, \tag{11}$$

where P_0, F_0 are constants to be determined. Note that in contrast to the case with $\Lambda = 0$, the gauge and Higgs field functions decay power-like and not exponentially.

2. For $R_1 < 0$, $R_2 < 0$, which turns out to be the most relevant case since we expect $L \gg 1$, i.e., the cosmological constant to be much smaller than the square of the Higgs boson mass from astrophysical observations, we have instead

$$P(x \gg 1) = P_0 x^{-1/2} \sin(\sqrt{-R_1/2} \log x + \phi_1), \tag{12}$$

$$f(x \gg 1) = 1 - F_0 x^{-3/2} \sin(\sqrt{-R_2/2} \log x + \phi_2) \tag{13}$$

where P_0, F_0 and ϕ_1, ϕ_2 are constants. We see in particular that both the gauge and Higgs field functions develop oscillations for $x \gg 1$.

3. For $R_1 > 0$, $R_2 < 0$ the gauge field behaves like in (10) and the Higgs field like in (13).

4. For $R_1 < 0$, $R_2 > 0$ the gauge field behaves like in (12) and the Higgs field like in (11).

4. Numerical results

Because Eqs. (4), (5) do not, to our knowledge, admit explicit solutions, we have solved them numerically using the ODE solver COLSYS [18].

Studying the equations numerically, we found that next to the natural deformations of the standard Abelian Higgs strings (which we call "fundamental string solutions" in the following), there exist solutions for which the Higgs field function vanishes at some intermediate value of the radial coordinate between the origin and the cosmological horizon. The scalar field function thus develops nodes. In the following, we will discuss these two different types of solutions and index them by the number k of nodes. The fundamental solution thus corresponds to $k = 0$.

4.1. Fundamental string solutions

First, we have constructed solutions corresponding to $n = 1$.

As a first step, we have chosen to find a solution with $R_1 < 0$ and $R_2 < 0$ (which we believe is the physically most relevant case). We have thus chosen $L = 3$, i.e., $R_2 = -27$ and $\alpha = 2$, i.e., $R_1 = -144$. The solution is shown in Fig. 1. In order to see the asymptotic behaviour predicted in (12) and (13), we plot the quantities $P(x)x^{1/2}$ and $(1 - f(x))x^{3/2}$. The oscillations for $x > L$ are then apparent.

We also present a $n = 1$-solution for $R_1 > 0$ and $R_2 < 0$ in Fig. 2. We have chosen again $L = 3$, but this time $\alpha = 0.01$, i.e., $R_1 = 0.28$. The oscillation in the scalar field is apparent when plotting $(1 - f(x))x^{3/2}$, while it is obvious from the plotted quantity $xP'(x)/P(x)$ that the gauge field is behaving power-like as in (10). Note that $xP'(x)/P(x)$ tends to a constant ~ -0.23 for $x \to \infty$.

We would like to stress that in both cases this correct asymptotic behaviour was NOT imposed as boundary condition, but was found numerically by imposing the appropriate conditions at the horizon.

The energy density T_0^0 of a typical de Sitter string solutions with $n = 1$, $L = 10$, $\alpha = 2$ and $\alpha = 0.5$, respectively, is shown in Fig. 3 (the $k = 0$ curves). Apparently, the energy density is peaked around $x = 0$ for the fundamental string. The corresponding inertial mass per unit length M_{in} for this solution is $M_{in}/(2\pi\eta^2) \approx$
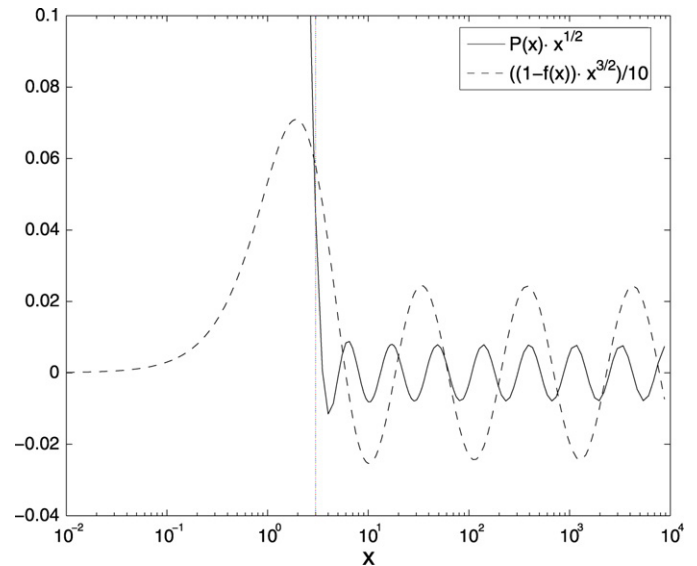

Fig. 1. The profiles of the quantities $P(x)x^{1/2}$ and $((1 - f(x))x^{3/2})/10$ are shown for a de Sitter string with $L = 3$ and $\alpha = 2$. The localisation of the horizon at $x = L = 3$ is also indicated.
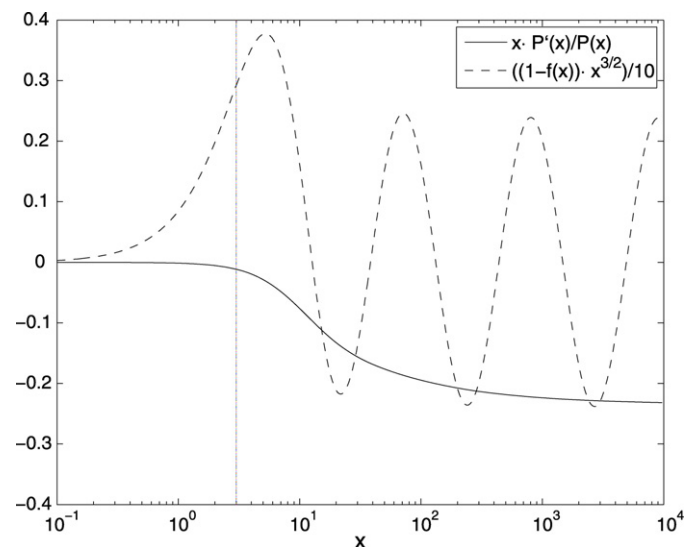

Fig. 2. The profiles of the quantities $xP'(x)/P(x)$ and $(1 - f(x))x^{3/2}/10$ are shown for a de Sitter string with $L = 3$ and $\alpha = 0.01$. The location of the cosmological horizon at $x = 3$ is also indicated.

0.75 for $\alpha = 2$ and $M_{in}/(2\pi\eta^2) \approx 0.99$ for $\alpha = 0.5$, respectively. We observe that when increasing L, the inertial mass increases and reaches the well-known values for $L \to \infty$, i.e., in the flat space–time limit. Note that $\alpha = 0.5$ corresponds to the self-dual limit. We would thus expect that $M_{in}/(2\pi\eta_2) \to 1$ for $\alpha = 0.5$ and $L \to \infty$. This is indeed what we find numerically.

One could then ask whether solutions with a power-like behaviour of the Higgs field ($R_1 < 0$ and $R_2 > 0$) or even solutions with a power-like behaviour of both the gauge and Higgs field ($R_1 > 0$ and $R_2 > 0$) are possible. We will show in the following that solutions of this type do not exist—at least in our numerical study they do not and we believe that we have constructed all possible de Sitter string solutions.

Let us explain this in more detail. In order to understand the solutions, we have studied their domain of existence in the α–L plane. One would expect that some sort of limiting behaviour exists, namely when $\Lambda \propto 1/L^2$ becomes comparable to the two other mass scales in the theory, i.e., M_H^2 and M_W^2.
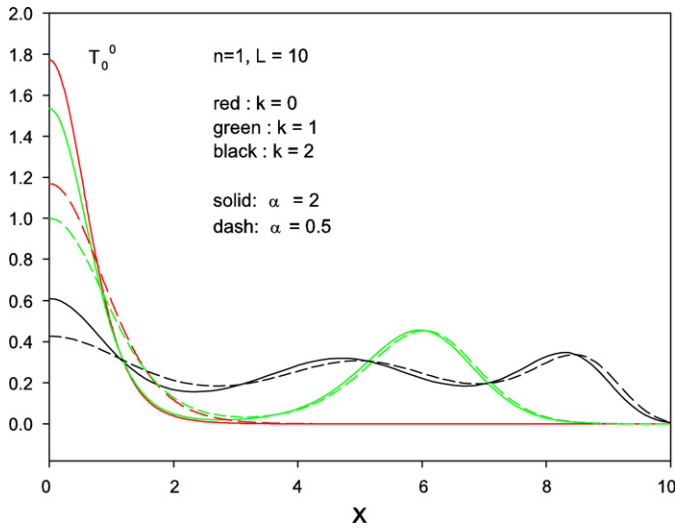
Fig. 3. The energy density T_0^0 inside the cosmological horizon is shown for $k = 0$, $k = 1$, $k = 2$. $k = 0$ corresponds to the fundamental solution, $k = 1$ and $k = 2$ to the first and second radially excited solutions, respectively. Here, we have chosen $n = 1$, $L = 10$, $\alpha = 2$ (solid) and $\alpha = 0.5$ (dashed), respectively. (For interpretation of the references to colour in this figure, the reader is referred to the web version of this Letter.)

Fig. 4. The quantities $P(L)$ and $f(L)$ are plotted as functions of L for $\alpha = 2$ (black) and $\alpha = 0.1$ (red). (For interpretation of the references to colour in this figure legend, the reader is referred to the web version of this Letter.)

Fig. 5. The quantities $-P'(L)$ and $f'(L)$ are plotted as functions of L for $\alpha = 2$ (black) and $\alpha = 0.1$ (red). (For interpretation of the references to colour in this figure legend, the reader is referred to the web version of this Letter.)

Let us first mention that—fixing $\alpha > 0$—we were able to construct solutions which approach the corresponding well-known string solution in flat space–time for $L \to \infty$, i.e., $\Lambda \to 0$. Accordingly we find for the values of the matter field functions and their derivatives at the cosmological horizon $P(L)$, $f(L)$, $P'(L)$, $f'(L)$: $P(L \to \infty) \to 0$, $f(L \to \infty) \to 1$, $P'(L \to \infty) \to 0$ and $f'(L \to \infty) \to 0$—irrespectively of the value of α. Decreasing the radius L, we find a branch of de Sitter strings which extends smoothly for the flat space–time limit with $P(L) > 0$, $f(L) < 1$, $P'(L) > 0$ and $f'(L) > 0$. This branch extends all the way back to a minimal value of the horizon radius at $L = L_{\min}(\alpha, n) > 0$. This is shown in Figs. 4, 5. E.g., for $n = 1$, we find $L_{\min} \approx 2.725$ for $\alpha = 1$ and $L_{\min} \approx 2.572$ for $\alpha = 2$. $L_{\min}$ thus decreases with increasing α. The explanation is obvious: when α is increased, the core radius of the string solution decreases and thus the de Sitter radius can also be decreased before it becomes comparable to the core radius.

For large values of α, we find that a second branch of de Sitter strings exists which extends back to a critical value of the horizon radius $L = L_{cr}$ at which it bifurcates with the trivial solution $P(x) = 1$, $f(x) = 0$. This is shown in Figs. 4, 5 for $\alpha = 2$. The existence of the two branches can be explained as follows. Since L is defined as $L = \sqrt{\beta}\eta l$, the variation of L can either be understood as fixing l and varying $\sqrt{\beta}\eta$, i.e., the Higgs boson mass, or by fixing $\sqrt{\beta}\eta$ and varying l. The limit $L \to \infty$ on the first branch corresponds to the flat space–time background with $l \to \infty$. In flat space–time and $\sqrt{\beta}\eta$ fixed string solutions with a well-defined core radius that is inversely proportional to $\sqrt{\beta}\eta$ exist. Decreasing l, i.e., increasing the cosmological constant, a branch of de Sitter string solutions exists. These solutions describe strings with a well-defined core radius inside a cosmological horizon. l can be decreased down to where it becomes comparable to the core radius. This point corresponds to the minimal value of L, $L_{\min}$. From there, a second branch of solutions exists, on which l is kept fixed while $\sqrt{\beta}\eta$ is varied up to L_{cr}. This works as long as the core radius is larger or comparable to the radius of the corresponding magnetic flux tube that is given by the inverse of the gauge boson mass. For smaller values of α, i.e., when the radius of the magnetic flux tube is larger than the core radius, no second branch exists and the branch of de Sitter solutions bifurcates with the
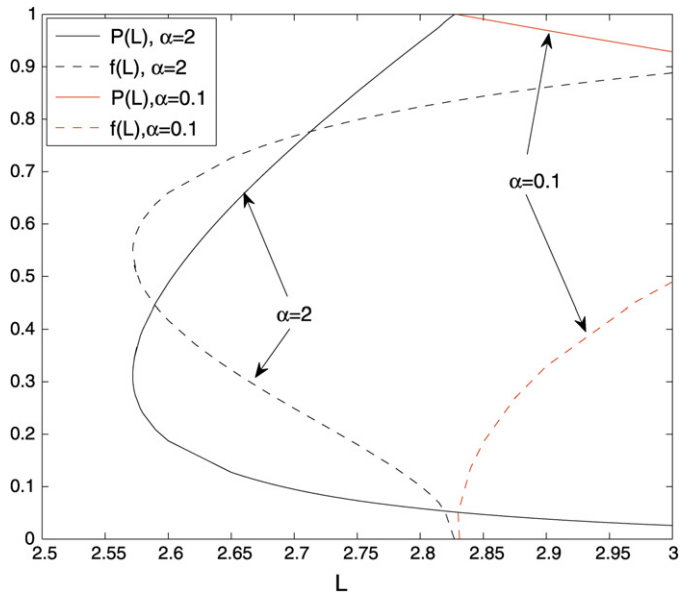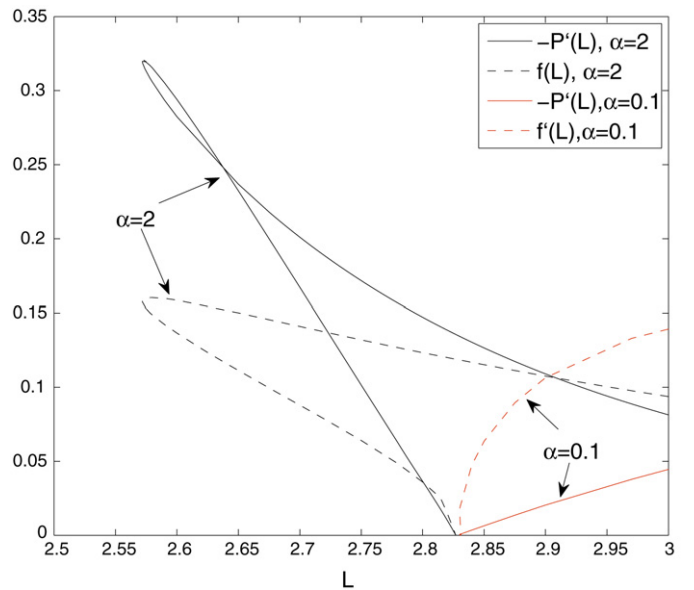
trivial solution at $L = L_{\min} = L_{cr}$. Decreasing L in this case, the cosmological horizon "sees" the magnetic flux tube first, since the core of the string lies within the flux tube. Since the variation of L can result from the variation of the Higgs boson mass, but not from the variation of the gauge boson mass at fixed l, there is no possibility for a second branch in this case. Interestingly, our numerical results indicate that L_{cr} depends only slightly on α. We find $L_{cr} \approx 2.83$.

In Fig. 6, we show the dependence of $L_{\min}$ and L_{cr} on α. We find that $L_{\min}$ becomes equal to L_{cr} at $\alpha \approx 0.466$. Note that de Sitter string solutions exist only in the parameter domain above the solid line. While solutions that fulfill the bound $R_1 = 1 - 8\alpha L^2 > 0$, i.e., have power-like decaying gauge fields are possible, **no** solutions with $R_2 = 9 - 4L^2 > 0$, i.e., $L < 3/2$ exist. Thus, all de Sitter strings have an oscillating Higgs field function outside the cosmo-
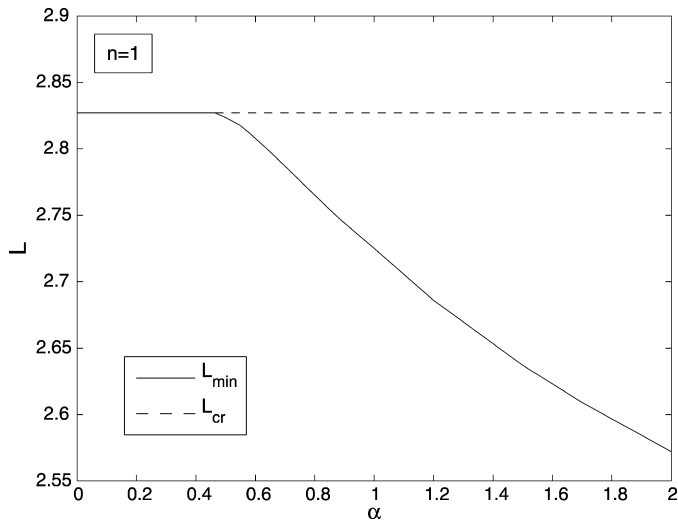
Fig. 6. The domain of existence of de Sitter strings is shown in the α–L plane. Plotted are the value of $L_{\min}$, the minimal possible value of the de Sitter radius in dependence on α, the square of the ratio of the gauge to Higgs boson mass. Also shown is the critical value of l, l_{cr}, where the solutions become trivial $P(x < \infty) = 1$ and $f(x < \infty) = 0$. Note that solutions exist only above the solid line.
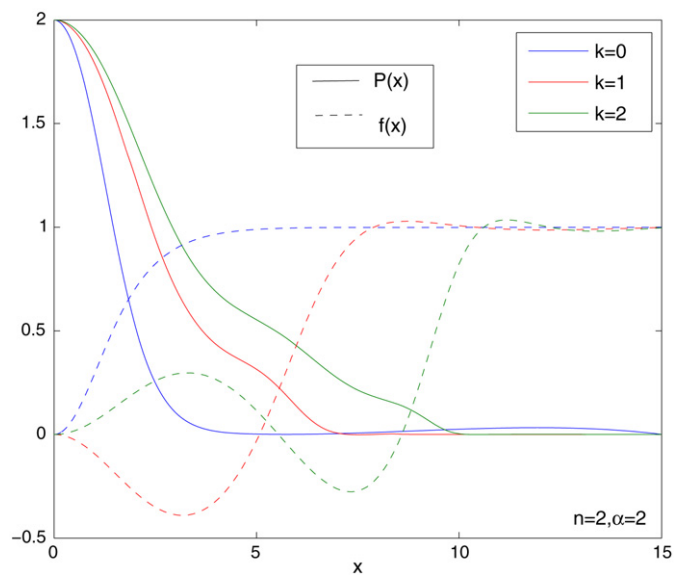

Fig. 7. We show the profiles of the gauge field function $P(x)$ (solid) and of the Higgs field function $f(x)$ (dashed) of the fundamental ($k = 0$, blue), the 1 excited ($k = 1$, red) and 2 excited ($k = 2$, green) $n = 2$ solution, respectively. Here, $\alpha = 2$ and $L = 7$ for $k = 0$, $k = 1$, while $L = 9$ for $k = 2$. (For interpretation of the references to colour in this figure legend, the reader is referred to the web version of this Letter.)

logical horizon. We believe that we have constructed all possible de Sitter strings and that no "isolated" branches exist in the α–L plane.

We have also studied higher winding solutions. In Fig. 7, we present the profiles of a solution for $n = 2$ and $\alpha = 2$ (blue curves). The study of the dependence of the solutions on α and L leads to a similar pattern as in the $n = 1$ case. We observe that for fixed α the minimal value of the horizon radius increases with n, e.g., we find $L_{\min}(\alpha = 2, n = 2) \approx 3.460$, while $L_{\min}(\alpha = 2, n = 1) \approx 2.572$ (see previous discussion). This is related to the fact that the $n = 2$ solution has a larger core radius as compared to the $n = 1$ solution.

We believe that the qualitative features are similar for $n \geqslant 3$, this is why we do not discuss them here.

4.2. Radially excited solutions

As mentioned above, our numerical results strongly suggest that new types of solutions exist in the presence of a positive cosmological constant. These solutions are characterized by nodes of the Higgs field function and can be interpreted as radially excited solutions of the fundamental string solutions discussed in the previous subsection. Here we present our results for solutions with one and two nodes. We believe that these are the first members of a tower of solutions labelled by the number of nodes $k \geqslant 1$ of the function $f(x)$. Note that with this notation the $k = 0$ solution corresponds to the fundamental solution discussed above.

The comparison of a $k = 0$, $k = 1$ and $k = 2$ solution is given for $n = 2$, $\alpha = 2$ and $L = 7$ for $k = 0$, $k = 1$, while $L = 9$ for $k = 2$ in Fig. 7. We observe that the function $f(x)$ of the $k = 1$ solution first decreases, reaches a minimum and then crosses zero before reaching its asymptotic value. Note that the value of the radial coordinate $x = x_0$ at which $f(x_0) = 0$ ($x_0 \approx 5.05$ for the solution shown in Fig. 7) is smaller than the corresponding L. The gauge field function $P(x)$ remains monotonically decreasing, but develops a "shoulder" in the region of x_0. Moreover, the radius of the core of the excited solution is larger than that of the fundamental solution. Similarly, the function $f(x)$ of the $k = 2$ solution reaches its asymptotic value after crossing the x-axis twice, while the gauge field function $P(x)$ develops two shoulders at the respective zeros of the function $f(x)$. We have not studied the critical behaviour of the $k = 2$ solution in detail, but we believe that it is qualitatively equal to the $k = 0$ and $k = 1$ cases.

We also show the energy density T_0^0 of the $k = 1$ and $k = 2$ radially excited solutions in Fig. 3. Here $n = 1$, $L = 10$, $\alpha = 2$ and $\alpha = 0.5$, respectively. Clearly, for the excited solutions, T_0^0 develops local maxima around the radii corresponding to the nodes of the function f.

For $k = 1$, we find $M_{\mathrm{in}}/(2\pi\eta^2) \approx 6.91$ for $\alpha = 2.0$ and $M_{\mathrm{in}}/(2\pi\eta^2) \approx 7.15$ for $\alpha = 0.5$, respectively. As expected, the mass inside the cosmological horizon of the excited solution is higher than the mass of the fundamental, i.e., $k = 0$ solution. Equally, one would expect that the mass of the excited solutions with more than one node of the Higgs field function is even higher. This is confirmed by our data for $k = 2$: we find $M_{\mathrm{in}}/(2\pi\eta^2) \approx 11.21$ for $\alpha = 2.0$ and $M_{\mathrm{in}}/(2\pi\eta^2) \approx 11.44$ for $\alpha = 0.5$, respectively.

Since radially excited solutions do not exist for the flat space–time limit it is natural to study the evolution of the solutions in terms of L and α, especially for $L \to \infty$. For this, we present the profiles of $f(x)$ for increasing L in Fig. 8.

The numerical results given in Fig. 8 suggest that the minimal value of $f(x)$ tends to -1 in the limit $L \to \infty$ and that the value of x_0 tends to infinity. Thus for $L \to \infty$, the solution approaches the corresponding Higgs field function of the Abelian string tending monotonically from 0 to -1. (Note that normally the Higgs field function of the Abelian string tends from 0 to 1, but that the equations of motion are invariant under $f \to -f$.)

A detailed analysis of the excited solution in the limit $L \to \infty$ is not aimed at in this Letter. Within the accuracy of our numerical results, it seems that, for a sufficiently large L, the function $|f|$ attains a maximum $|f(x_m)| = 1$ at a relatively small value of $x = x_m$ (i.e., with $x_m/L \ll 1$) and that $|f(L)| = 1$. In the interval $x \in [x_m, L]$, we have $P(x) \sim 0$ while $f(x)$ develops several oscillations. The investigation of a relation between the corresponding equation for f and some special function is currently underway.

We have also studied the critical behaviour of the $k = 1$ solutions and found a qualitatively similar pattern as for the $k = 0$ case.

In Fig. 9, we show the values of the gauge field and Higgs field functions at the cosmological horizon $P(L)$ and $f(L)$, respectively, as functions of L for $\alpha = 2$ and $\alpha = 0.1$. Here, we have chosen
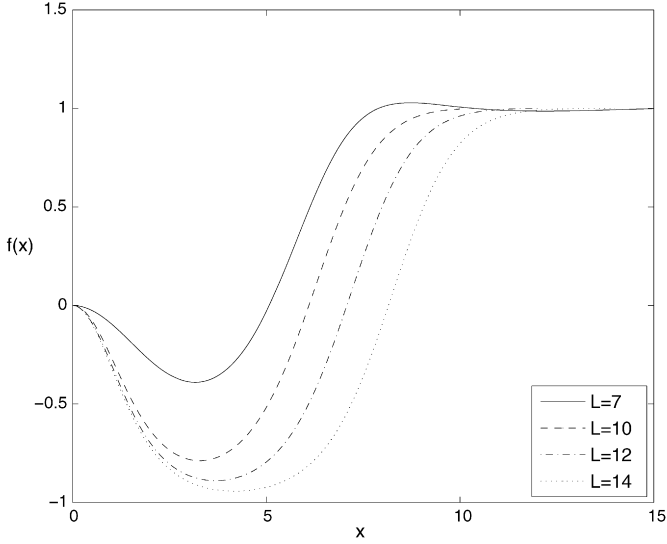
Fig. 8. The profiles of the Higgs field function $f(x)$ of the 1 excited solution are shown for $n = 2$, $\alpha = 2$ and different values of L.
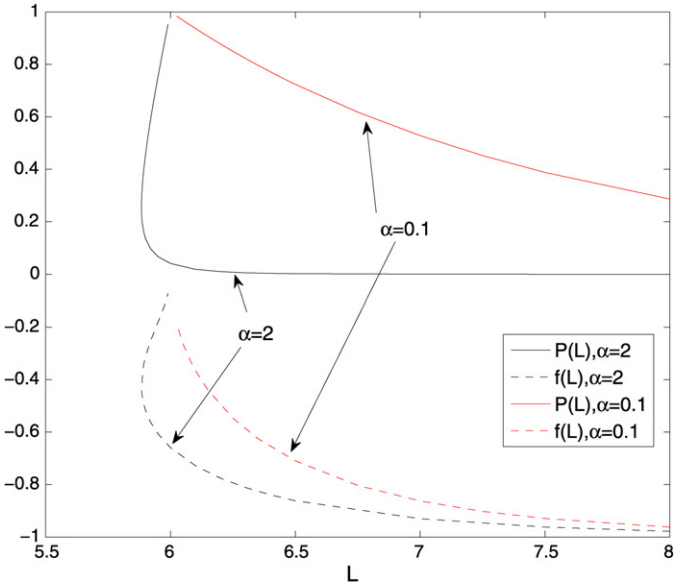

Fig. 9. The values of the gauge and Higgs field functions at the horizon, $P(L)$ and $f(L)$, respectively, are shown as functions of L for $\alpha = 2$ (black) and $\alpha = 0.1$ (red). Here $n = 1$ and $k = 1$. (For interpretation of the references to colour in this figure legend, the reader is referred to the web version of this Letter.)

$n = 1$. Again, the radially excited solutions bifurcate with the trivial solution $P(x) \equiv n$ and $f(x) \equiv 0$ at a critical value of L: $L_{cr}(\alpha, n)$. We find $L_{cr}(\alpha, n = 1) \approx 6$, where our numerical results indicate that L_{cr} depends very weakly on α.

For small values of α, the critical value is attained directly by decreasing L, while for larger α, a second branch of solutions exists that extends backwards from a minimal value of the cosmological horizon radius L_{min} with $L_{min}(\alpha = 2, n = 1) \approx 5.885$.

In Fig. 10, we show the profiles of the $k = 1$ solution for $n = 1$, $\alpha = 2$ and different values of L along the two branches. $L = 12$ (blue) corresponds to a solution on the first branch and the oscillations of the functions outside the cosmological horizon are so small that they are not apparent in the plot. The case $L = 5.885$ (green) corresponds to the minimal value of L for this choice of n and α. Here, the amplitude of the oscillations of the fields outside the horizon are larger and can be seen in the figure. Finally, we also present a solution on the second branch, very close to the
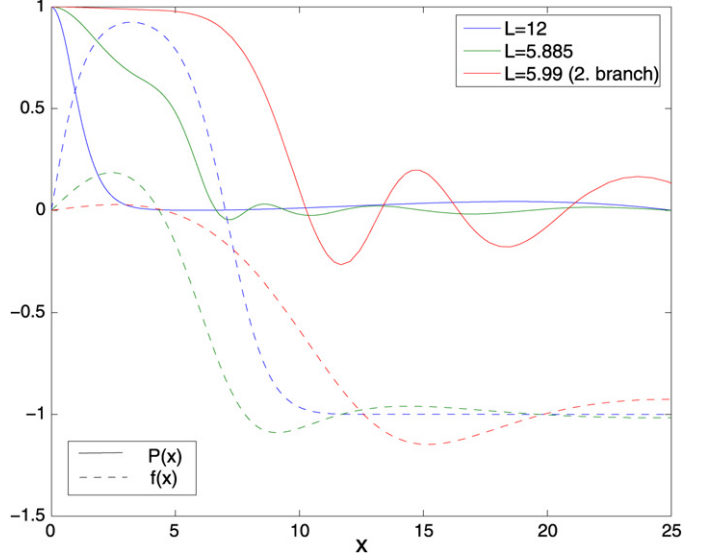

Fig. 10. The profiles of the gauge and Higgs field functions $P(x)$ and $f(x)$ are shown for three different values of L and $\alpha = 2$, $k = 1$, $n = 1$. (For interpretation of the references to colour in this figure, the reader is referred to the web version of this Letter.)

critical value of L at $L = 5.99$ (red). Here, both $P(x)$ as well as $f(x)$ deviate only slightly from their values at the origin inside the horizon, while outside the horizon, they reach their asymptotic values after large amplitude oscillations around these values.

5. Deficit angle

In all our numerical calculations, we have assumed the de Sitter background to be fixed. To study the full dynamical space–time is very difficult since the resulting equations are partial differential equations. In [17], an approximation for weak gravitational fields was used to study the effects of a string on anti-de Sitter space–time. In that case, the Einstein equations can be linearized. We employ this method here for the de Sitter case. The metric used reads [17]

$$ds^2 = \exp(2z/l)\left(-\exp(A)\, d\hat{t}^2 + d\hat{\rho}^2 + F^2\, d\varphi^2\right) + \exp(C)\, dz^2, \quad (14)$$

where A, F and C are functions of $\hat{\rho}$ and z. Introducing the rescaled coordinate $\hat{x} = \sqrt{\beta}\eta\hat{\rho}$, letting $z \to \sqrt{\beta}\eta z$, $t \to \sqrt{\beta}\eta t$ and assuming that the functions depend only on the combination $x = \hat{x}\exp(z/L)$, the linearized Einstein equation for F reads

$$\frac{2}{L^2} + \frac{1}{F}\frac{d}{dx}\left(\left(1 - \frac{x^2}{L^2}\right)\frac{dF}{dx}\right) = \gamma T_0^0, \quad (15)$$

where $\gamma = 8\pi G$ and T_0^0 is the energy–momentum tensor of the string in the de Sitter background (8). The deficit angle δ of the space–time is then given by $\delta = 2\pi(1 - F'|_{x=x_0})$, where we choose $x_0 < L$.

Outside the core of the string where $T_0^0 = 0$, we find as solutions to (15)

$$F = c_1 y + c_2\left(\frac{1}{2}y\log\left(\frac{1+y}{1-y}\right) - 1\right), \quad (16)$$

where $y := x/L$ and c_1 and c_2 are constants to be fixed by the boundary conditions of F at the origin. Note that (within the linearized approximation) the function $F(y)$ becomes singular for $y \to 1$, i.e., at the cosmological horizon $x = L$, if $c_2 \neq 0$. Integrating the above equation for our solutions, we find that the function $F'(y)$ develops a plateau inside the cosmological horizon if L is large enough. This signals that the space–time inside the cosmological horizon has a deficit angle. We observe that this deficit

angle increase with the decrease of L. Choosing $x_0 = L/2$ and integrating (15) we find the following approximated behaviour of the deficit angle from our numerics

$$\delta \approx \gamma M_{\text{in}} \left(1 + \frac{8}{3L^2}\right). \qquad (17)$$

In astrophysical observations it has thus to be taken into account that the presence of a positive cosmological constant tends to increase the deficit angle as compared to asymptotically flat-space–time. The separation between two lensed objects would thus increase with increasing cosmological constant.

6. Conclusions

We have studied Abelian Higgs strings in a fixed de Sitter background. While these solutions have already been discussed in [15], we find new features of the solutions here and especially study the behaviour of the matter field functions outside the cosmological horizon. We find that all possible de Sitter strings have oscillating Higgs fields outside their horizon. This observation is important when calculating the mass of these solutions using the so-called counterterm method [19]. For this, we would have to couple the Abelian Higgs model minimally to gravity. However, in that case, the differential equations would not reduce to ordinary differential equations (like in our case), but one would have to solve the "full" partial differential equations. Since it was observed for magnetic monopoles, that the background limit is qualitatively comparable to the fully coupled case [16], we believe that if we would couple our model to gravity that the oscillating Higgs fields outside the horizon would still be a feature of the model. Like in the case of magnetic monopoles this would then lead to the conclusion that Abelian strings have diverging mass as evaluated at infinity. The verification of this statement is currently underway and is left for a future publication.

Moreover, we observe a new feature of the Abelian Higgs model: for non-vanishing cosmological constant, radially excited solutions exist. Interestingly, the Higgs field function has nodes in this case. We find that these excited solutions have inertial mass per unit length inside the cosmological horizon much larger than the fundamental string solutions.

Note added

Solutions that are oscillating have also been observed in the context of solid state physics [20]. Y.B. gratefully acknowledges J. Govaerts for bringing this reference to his attention.

Acknowledgements

References

[1] A. Vilkenin, E.P.S. Shellard, Cosmic Strings and Other Topological Defects, Cambridge Univ. Press, Cambridge, 1994;
T.W.B. Kibble, M. Hindmarsh, Rep. Prog. Phys. 58 (1995) 447;
T.W.B. Kibble, J. Phys. A 9 (1976) 1387;
Ya.B. Zel'dovich, Mon. Not. R. Astron. Soc. 192 (1980) 663;
A. Vilenkin, Phys. Rev. D 23 (1981) 852.
[2] See, e.g., L. Perivolaropoulos, Nucl. Phys. B (Proc. Suppl.) 148 (2005) 128, and references therein.
[3] G. Dvali, A. Vilenkin, JCAP 0403 (2004) 010;
E.J. Copeland, R.C. Myers, J. Polchinski, JHEP 0406 (2004) 013;
A. Achúcarro, J. Urrestilla, JHEP 0408 (2004) 050.
[4] N. Jones, H. Stoica, S.H.H. Tye, JHEP 0207 (2002) 051;
S. Sarangi, S.H.H. Tye, Phys. Lett. B 536 (2002) 185;
E.P. Copeland, R.C. Myers, J. Polchinski, JHEP 0406 (2004) 013;
J. Polchinski, hep-th/0412244;
A.C. Davis, T.W.B. Kibble, Contemp. Phys. 46 (2005) 313;
S.H.H. Tye, hep-th/0610221;
J. Polchinski, arXiv: 0707.0888;
M. Sakellariadou, arXiv: 0802.3379;
L. Kofman, A. Linde, A.A. Starobinsky, Phys. Rev. Lett. 76 (1996) 1011;
I. Tkachev, S. Khlebnikov, L. Kofman, A. Linde, Phys. Lett. B 440 (1998) 262;
R. Jeannerot, Phys. Rev. D 53 (1996) 5426;
R. Jeannerot, Phys. Rev. D 56 (1997) 6205;
R. Jeannerot, J. Rocher, M. Sakellariadou, Phys. Rev. D 68 (2003) 103514;
J. Rocher, M. Sakellariadou, Phys. Rev. Lett. 94 (2005) 011303;
E.J. Copeland, A.R. Liddle, D.H. Lyth, E.D. Stewart, D. Wands, Phys. Rev. D 49 (1994) 6410;
R. Jeannerot, hep-ph/0610295;
G. Dvali, A. Vilenkin, JCAP 0403 (2004) 010;
E.J. Copeland, R.C. Myers, J. Polchinski, JHEP 0406 (2004) 013;
N. Barnaby, A. Berndsen, J.M. Cline, H. Stoica, JHEP 0506 (2005) 075;
H. Firouzjahi, S.H.H. Tye, JCAP 0503 (2005) 009;
S.E. Shandera, S.-H.H. Tye, JCAP 0605 (2006) 007;
R. Bean, S.E. Shandera, S.H.H. Tye, J. Xu, JCAP 0705 (2007) 004.
[5] C. Contaldi, M. Hindmarsh, J. Magueijo, Phys. Rev. Lett. 82 (1999) 2034;
R.A. Battye, J. Weller, Phys. Rev. D 61 (2000) 043501;
F.R. Bouchet, P. Peter, A. Riazuelo, M. Sakellariadou, Phys. Rev. D 65 (2002) 21301;
N. Bevis, M. Hindmarsh, M. Kunz, Phys. Rev. D 70 (2004) 043508, astro-ph/0403029;
M. Wyman, L. Pogosian, I. Wasserman, Phys. Rev. D 72 (2005) 023513;
M. Wyman, L. Pogosian, I. Wasserman, Phys. Rev. D 73 (2006) 089905, Erratum;
M. Landriau, E.P.S. Shellard, Phys. Rev. D 69 (2004) 023003;
M. Landriau, E.P.S. Shellard, JCAP 0409 (2004) 008;
E. Jeong, G.F. Smoot, astro-ph/0406432;
J.-H.P. Wu, astro-ph/0501239;
U. Seljak, A. Slosar, P. McDonald, JCAP 0610 (2006) 014;
N. Bevis, M. Hindmarsh, M. Kunz, J. Urrestilla, Phys. Rev. Lett. 100 (2008) 021301;
R.A. Battye, B. Garbrecht, A. Moss, H. Stoica, arXiv: 0710.1541 [astro-ph];
L. Pogosian, S.H.H. Tye, I. Wasserman, M. Wyman, arXiv: 0804.0810 [astro-ph].
[6] H.B. Nielsen, P. Olesen, Nucl. Phys. B 61 (1973) 45.
[7] P.M. Saffin, JHEP 0509 (2005) 011;
A. Rajantie, M. Sakellariadou, H. Stoica, JCAP 0711 (2007) 021;
M. Sakellariadou, H. Stoica, arXiv: 0806.3219.
[8] D. Garfinkle, Phys. Rev. D 32 (1985) 1323;
M. Christensen, A.L. Larsen, Y. Verbin, Phys. Rev. D 60 (1999) 125012;
Y. Brihaye, M. Lubo, Phys. Rev. D 62 (2000) 085004.
[9] A. Vilenkin, Astrophys. J. 282 (1984) L51;
A. Vilenkin, Phys. Rep. 121 (1985) 263;
A. Vilenkin, Nature 322 (1986) 613.
[10] S. Perlmutter, et al., Astrophys. J. 517 (1999) 565;
A.G. Riess, et al., Astron. J. 116 (1998) 1009.
[11] M.R. Anderson, The Mathematical Theory of Cosmic String—Cosmic Strings in the Wire Approximation, IOP Publishing, 2003;
A.L. Larsen, Phys. Rev. D 50 (1994) 2623;
Z. Gu, H. Cheng, Gen. Relativ. Gravit. 39 (2007) 1;
Y. Liu, H. Cheng, arXiv: 0801.4615.
[12] A. Strominger, JHEP 0110 (2001) 034;
A. Strominger, JHEP 0111 (2001) 049.
[13] B. Linet, J. Math. Phys. 27 (1986) 1817;
H.J. Vega, N.G. Sanchez, Phys. Rev. D 47 (1993) 3394.
[14] E.R. Bezerra de Mello, Y. Brihaye, B. Hartmann, Phys. Rev. D 67 (2003) 124008.
[15] A.M. Ghezelbash, R.B. Mann, Phys. Lett. B 537 (2002) 329;
A.M. Ghezelbash, R.B. Mann, AIP Conf. Proc. 646 (2003) 223.
[16] Y. Brihaye, B. Hartmann, E. Radu, Phys. Rev. Lett. 96 (2006) 071101;
Y. Brihaye, B. Hartmann, E. Radu, C. Stelea, Nucl. Phys. B 763 (2007) 115.
[17] M.H. Dehghani, A.M. Ghezelbash, R.B. Mann, Nucl. Phys. B 625 (2002) 389.
[18] U. Ascher, J. Christiansen, R.D. Russell, Math. Comput. 33 (1979) 659;
U. Ascher, J. Christiansen, R.D. Russell, ACM Trans. 7 (1981) 209.
[19] V. Balasubramanian, J. de Boer, D. Minic, Phys. Rev. D 65 (2002) 123508.
[20] J. Govaerts, G. Stenuit, D. Bertrand, O. van der Aa, Phys. Lett. A 267 (2000) 56.